Nova Biotechnol Chim (2022) 21(1): e1023
DOI: 10.36547/nbc.1023

Nova Biotechnologica *et* Chimica

Ag/SiO_2 nanocomposite mediated by *Escherichia coli* D8 and their antimicrobial potential

Mohamed M. El-Zahed✉, M. I. Abou-Dobara, Ahmed K.A. El-Sayed, Zakaria A. M. Baka

Department of Botany and Microbiology, Faculty of Science, Damietta University, New Damietta, Egypt

✉Corresponding author: *mohamed.marzouq91@du.edu.eg*

Article info

Article history:
Received: 20th June 2021
Accepted: 8th November 2021

Keywords:
Antimicrobial
Biosynthesis
Escherichia coli
Nanocomposite
Silica
Silver

Abstract

Silica (SiO_2) has a fundamental role in the recuperation of plants in response to environmental stresses, besides the induction of resistance against plant diseases. Silver nanoparticles (AgNPs) have a superior antimicrobial activity. The combination between SiO_2 and AgNPs is a promising approach due to their antimicrobial activity, biological activity, low toxicity, and high stability of the produced nanocomposite. The current study postulated a green method for silver/silica nanocomposite (Ag/SiO_2NC) synthesis at room temperature using the crude metabolites of *Escherichia coli* D8 (MF062579) strain in the presence of sunlight. UV-Vis spectrophotometry, X-ray diffraction (XRD), Fourier transform-infrared spectroscopy (FTIR), and transmission electron microscopy (TEM) analyses have characterized the biosynthesized nanocomposite. TEM study of Ag/SiO_2NC showed an average particle size of ~32 – 48 nm whereas AgNPs showed a mean size of 18 – 24 nm. The negative charged Ag/SiO_2NC (-31.0 mV) showed potent antimicrobial activity against *Bacillus cereus* ATCC6633, *Klebsiella pneumoniae* ATCC33495, *Staphylococcus* aureus (ATCC25923), *E. coli* (ATCC25922), *Candida albicans* (ATCC10231), and *Botrytis cinerea* (Pers: Fr.). The minimum inhibitory concentration (MIC) test showed a dose-dependent manner of Ag/SiO_2NC antimicrobial action. MIC values of Ag/SiO_2NC against the tested pathogens exhibited 125 and 6.25 $\mu g.mL^{-1}$ as antibacterial and antifungal agents, respectively. TEM micrographs showed changes in the pathogens treated with Ag/SiO_2NC including wrinkling, damage, and rupture of the bacterial cell membrane. In addition, the formation of a mucilage matrix connecting the hyphal cells, the appearance of big vacuoles and lipid droplets with severe leakage of cytoplasmic contents of the treated *B. cinerea* were also recorded.

Introduction

Nowadays, there is a tendency to use materials after converting them into their nano-form, because of the new and promising advantages and unique properties gained in the new nano-form such as antimicrobial activity, chemical, magnetic, electronic, or mechanical properties because of the change of quantum and surface boundary effects compared with their bulk materials (Chhipa and Joshi 2016; Musere *et al.* 2021). Nanomaterials can be described as materials with a size of 1 – 100 nm, known as the nano-scale range. Synthesis of nanometals can be done using different methods such as chemical, physical or biological techniques. Conventional hypothesis of chemical synthesis of nanoparticles (NPs) might possess several serious problems due to using expensive toxic chemicals (Zhang *et al.* 2021).

Physical methods include high radiation and stabilizing agents that might be dangerous for human health and to the environment (Awwad *et al.* 2020). Accordingly, the green synthesis of NPs by plant extracts or microbial metabolites plays an important role in the reduction of metal ions into NPs and capping them in supporting their stability (Parveen *et al.* 2016). Biological NPs have different characters compared with chemical or physical NPs, with superior stability and suitable dimensions due to the one-step technique (Narayanan and Sakthivel 2011).

Silver nanoparticles (AgNPs) were used as a potent antimicrobial agent during the last decades (Hamad *et al.* 2020). It showed antimicrobial activity against pathogens such as *Escherichia coli* (Yang *et al.* 2021), *Staphylococcus aureus* (Enan *et al.* 2021), *Klebsiella pneumoniae* (Pareek *et al.* 2021), *Candida albicans* (Takamiya *et al.* 2021), and *Botrytis cinerea* (Ouda 2014). The aggregation of AgNPs is a common problem that decreases their biological activity (El-Dein *et al.* 2021). One way to enhance the metal NPs stability is by stabilizing them by embedding them inside a polymer, which prevents their aggregation, even at high-volume fractions (Baheiraei *et al.* 2012). Several previous studies have focused on the synthesis of stable monodisperse silica-coated with nanometals, mainly Ag and gold (Au) (Chen *et al.* 2017; Si *et al.* 2019; Li *et al.* 2021). Silica (SiO_2) can act as the platform for developing NPs moreover having antimicrobial properties owing to their large surface area, positive surface charge, and monodispersity. Gankhuyag *et al.* (2021) reported that SiO_2 might increase the stability of the nanometals and prevent their aggregation. In addition, the net positive charge of SiO_2 facilitates a greater number of AgNPs to interact with the negatively charged surface of bacteria, resulting in highly efficient antimicrobial activity (Jayasuriya 2017). Egger *et al.* (2009) and Sohrabnezhad *et al.* (2020) demonstrated the antibacterial activity of silver/silica nanocomposite (Ag/SiO_2NC) against both *E. coli* and *S. aureus*. Ag/SiO_2NC revealed marked changes in the bacterial cell contents, including the cell wall integrity, metabolism, and genetic stability of *Pseudomonas aeruginosa* (Anas *et al.* 2013). Also, Xu *et al.* (2009) reported the antibacterial effects of Ag/SiO_2 core-shell particles against *E. coli* and *S. aureus*. Ag/SiO_2NC had antifungal potential against *B. cinerea* as reported by Oh *et al.* (2006). Youssef and Roberto (2021) demonstrated the antifungal activity of chitosan/silica nanocomposite against *B. cinerea.* Ag/SiO_2NC showed fungicidal activity against the pathogenic fungi in the soybean plants (*Fusarium* oxysporum and *Rhizoctonia solani*) as reported by Nguyen *et al.* (2016) and *Aspergillus flavus* as reported by Diagne *et al.* (2020). Hence, new distinctive structures of Ag/SiO_2NC could present a new prospect for its antimicrobial activity.

The present study aimed to evaluate the ability of the crude metabolite of *E. coli* D8 (MF062579) for reducing the silver nitrate ($AgNO_3$) into AgNPs extracellularly and also their binding with SiO_2 in a new one-step green approach. The antimicrobial potential of Ag/SiO_2NC was studied against some pathogenic strains, comparing their activity to the standard commercial antibiotics.

Experimental

Microbial cultures

E. coli D8 (AC: MF062579) and the pathogenic bacterial and fungal strains were obtained from the culture collection of Botany and Microbiology Department, Faculty of Science, Damietta University, Egypt.

Chemicals

The chemicals included silver nitrate (Panreac Quimica S.L.U, Barcelona, Spain), silica (Silicon dioxide nanoparticles, particle size 190 – 250 nm, mesoporous, pore size 4 nm, Sigma-Aldrich), culture media, and other chemicals (Sigma Aldrich Chemical Pvt. Ltd., India). Penicillin G potassium (Buffered Pfizerpen) and fluconazole (Diflucan) were purchased from Pfizer Inc., New York, NY.

Biosynthesis of silver nanoparticles and silver/silica nanocomposite

Silver nanoparticles were prepared according to El-Zahed *et al.* (2021). In brief, *E. coli* D8 agar slants were sub-cultured on nutrient agar plates (37 °C, 24 h). Then the grown colonies were inoculated into a nutrient broth medium with 0.5 McFarland standard ($1 – 2 \times 10^8$ CFU.mL^{-1}) and incubated at

37 °C/150 rpm for 48 h. Later, the cell-free metabolites of *E. coli* D8 were collected by centrifugation (3H24RI intelligent high-speed refrigerated centrifuge, Herexi Instrument, and Equipment Co., Ltd) at 8,000 rpm for 20 min and filtration through a sterile 0.22 µm syringe filter (Millex GV, Millipore). For the synthesis of AgNPs, 1.5 mM of $AgNO_3$ solution was mixed with cell-free metabolites (1 % v/v) at room temperature and sunlight. For the synthesis of Ag/SiO_2NC, 0.5g of $AgNO_3$ was dissolved into 50 mL of distilled water and then added to another beaker that included 100 g of SiO_2. At room temperature, the previous solution was mixed well with 20 mL of *E. coli* D8 cell-free metabolites in the presence of sunlight.

The first indicator for the AgNPs and nanocomposite (NC) formation was the color change from colorless ($AgNO_3$) or white (SiO_2) into brown. After 20 min, the AgNPs and Ag/SiO_2NC were collected separately by centrifugation at 10,000 rpm for 15 min several times and then dried in an oven at 50 °C for 24 h. Then, the NPs and NC were dried at 185 °C for 5 h (Sadeghi *et al*. 2013).

Characterization of silver/silica nanocomposite

Silver/silica nanocomposite spectra were scanned by UV/VIS/NIR Spectrophotometer (V-630, JASCO Corporation, Japan). The X-ray diffraction (XRD) pattern of the Ag/SiO_2NC was performed at 2θ values (l = 1.54 °A in the range 10 – 80 °) using a Cu X-ray tube at 40 kV and 30 mA with the X-ray diffractometer (model LabX XRD-6000, Shimadzu, Japan). Fourier transform infrared spectroscopy (FTIR) spectrum of the Ag/SiO_2NC was recorded by JASCO FT/IR-4100typeA in the 400 – 4,000 cm^{-1} range. The size and morphology of AgNPs and Ag/SiO_2NC were investigated by TEM (JEOL, JEM-2100, Japan) at an accelerating voltage of 200 kV and using a carbon-coated copper grid (Type G 200, 3.05 µM diameter, TAAP, USA). Charge of AgNPs and size distribution by volume were recorded by Zeta Potential Analyzer (Malvern Zetasizer Nano-ZS90, Malvern, UK).

Antimicrobial potential

The antimicrobial potential of Ag/SiO_2NC was tested against Gram-positive bacteria (*S. aureus* ATCC25923 and *Bacillus cereus* ATCC6633), Gram-negative bacteria (*E. coli* ATCC25922 and *K. pneumoniae* ATCC33495), yeast (*C. albicans* ATCC10231), and the phytopathogenic fungus (*B. cinerea* Pers: Fr.) by agar well diffusion and broth dilution methods. The bacterial, yeast and fungal strains were grown and tested using Mueller Hinton agar (MHA), bacto-casitone agar, and potato dextrose agar (PDA) plates, respectively. 200 µL of 0.5 McFarland standard ($1 – 2 \times 10^8$ $CFU.mL^{-1}$) of microbial suspension was used as an initial inoculum for each test.

Agar well diffusion method

Agar well diffusion assay was performed *in vitro* against the microbial strains according to the guidelines of the Clinical and Laboratory Standards Institute (Clinical and Laboratory Standards 2006). About 200 µL of 150 $µg.mL^{-1}$ of SiO_2, Ag/SiO_2NC, $AgNO_3$, penicillin G potassium (antibacterial), and fluconazole (antifungal) were prepared and added separately into small wells (5 mm diameter of size) that were made into the solidified agar plates. Plates were incubated at 37 °C for 48 h, 30 °C for 48 h, or 28 °C for 5 days, for bacteria, yeast, and fungi, respectively. After the incubation period, inhibition zones were measured in millimeters (mm).

Broth dilution method

Mueller Hinton, bacto-casitone and potato dextrose broth media test tubes were prepared, autoclaved, and inoculated by 100 µL of microbial suspensions (0.5 McFarland standard ($1 – 2 \times 10^8$ $CFU.mL^{-1}$)) in three sets of test tubes containing different dosages of Ag/SiO_2NC and Penicillin G potassium (antibacterial) or fluconazole (antifungal) concentrations (6.25 – 125 $µg.mL^{-1}$). Then, the tubes were incubated at 37 °C/120 rpm for 24 h, 30 °C/120 rpm for 24 h, or 28 °C/120 rpm for 5 days, for bacteria, yeast, and fungi, respectively. The minimal inhibition concentration (MIC) for the tested pathogenic strains was determined by measuring their growth spectrophotometrically at

600 nm against negative controls (exclusive of Ag/SiO_2NC). The growth inhibition percentage was calculated using the following formula (Eq. 1):

$$\% \text{ Growth inhibition} = \left[\frac{ODc - ODt}{ODc} \times 100\right] \quad (1)$$

where the negative control (broth media exclusive of Ag/SiO_2NC) optical density; ODc and the Ag/SiO_2NC-treated tested sample optical density; ODt (Clinical and Laboratory Standards 2008; 2017).

Ultrastructural study

The ultrastructure of Ag/SiO_2NC treated *E. coli* and *B. cinerea* was studied with TEM (JEOL, JEM-2100, Japan, 200kV) according to Bozzola (2007). The tested strains were subjected to Ag/SiO_2NC (MIC, 6.25 µg.mL^{-1}) for 2 h and compared with untreated bacteria and fungi as controls. The samples were fixed in 2.5 % glutaraldehyde in 0.1M cacodylate buffer at pH 7.0 and then post-fixed in 1 % osmium tetroxide, dehydrated with a graded series of ethanol, embedded in a plastic resin, and sectioned on an ultramicrotome. Ultrathin sections were double-stained with uranyl acetate and lead citrate and then loaded on carbon-coated copper grids (Type G 200, 3.05 µM diameter, TAAP, U.S.A.).

Statistical analysis

SPSS software version 18 was used for all the statistical analysis. All values in the experiments were expressed as the mean ± standard deviation (SD) and were analyzed with a one-way Analysis of Variance (ANOVA) with a significant level set at $P < 0.05$.

Results and Discussion

Synthesis and characterization of Ag/SiO_2NC

Synthesis and characterization of Ag/SiO_2NC have attracted the attention of the materials community because of their promising properties (Zaferani 2018). The green synthesis approach of those NCs with controllable size and properties has applications in miniaturized catalysts, photonics, optical devices, medical applications moreover it could be used as a potential nanomicrobicide and nanoscale growth regulator in agriculture (Das *et al.* 2019). Endless progression of microbial antibiotic-resistant mechanisms claims continuous searching for alternative approaches to deal with their risk to humans and plants (Rai *et al.* 2012). The present study provided a green approach for the synthesis of antimicrobial Ag/SiO_2NC mediated by the cell-free metabolites of *E. coli* D8. FTIR spectrum confirmed the presence of proteins during the bio-reduction process. These proteins, in the *E. coli* D8 metabolite, might be including the reducing enzymes and/or some redox agents such as sulfur-containing proteins resulting in the bio-reduction of silver ions (Ag^+) into AgNPs (Krishnaraj *et al.* 2012). Also, quinones (menaquinone, demethylmenaquinone, and ubiquinone) found in the *E. coli* D8 metabolite act as an electron shuttle compound and reduced Ag^+ into AgNPs in the presence of sunlight as reported by Duan *et al.* (2015) and Sharma *et al.* (2012).
The biosynthesis of AgNPs was confirmed through visual observation of the color change of the mixture into brown color producing an obvious absorption peak at 430 nm (Fig. 1). The brown color is because of the excitation of the AgNPs surface plasmon resonance (El-Dein *et al.* 2021). Granbohm *et al.* (2018) found the UV-Vis spectra of Ag/SiO_2NC powders showed the silver SPR peak at 410 nm.

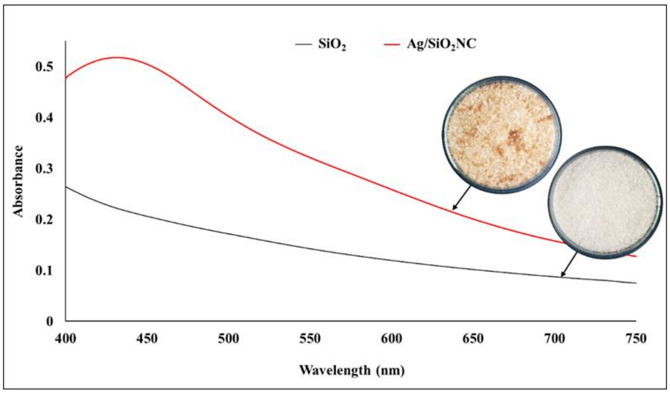

Fig. 1. The UV-Vis spectra of SiO_2 and Ag/SiO_2NC.

The XRD patterns of SiO_2 were examined and showed an amorphous SiO_2 characteristic diffraction peak at 22.4 °. Ag/SiO_2NC XRD pattern revealed peaks at 2θ angles of 32.25 °, 38.25 ° and 44.4 ° corresponding to the reflections of (110), (111) and (200) crystalline planes of the facecentered cubic (FCC) structure of AgNPs (Fig. 2). Also, we had found no other diffraction peaks for silver oxide in the Ag/SiO_2NC XRD pattern which showed the coverage of the NC with pure AgNPs (Xu *et al.* 2015).

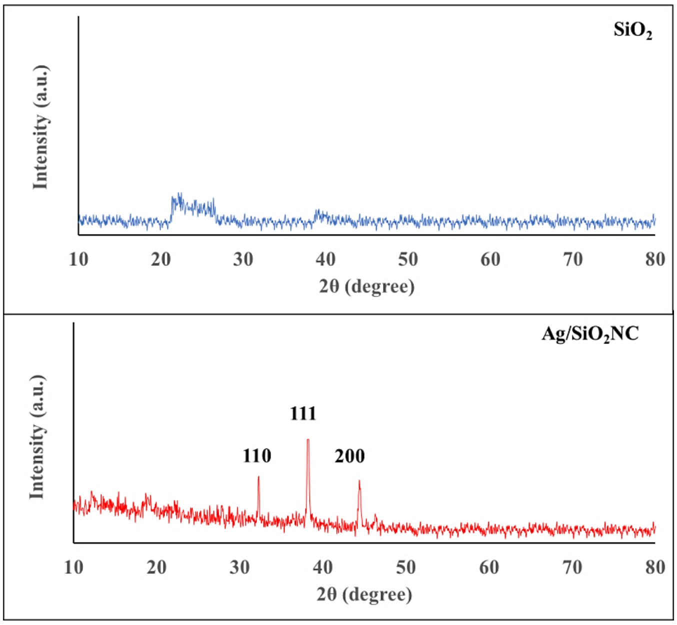

Fig. 2. The XRD patterns of SiO_2 and Ag/SiO_2NC.

The FTIR spectra of Ag/SiO_2NC were analyzed in the region of 400 – 4,000cm^{-1} (Fig. 3). The vibration bands around 3,431 and 1,613 cm^{-1} are attributed to the OH and carbonyl group (C=O), respectively. These signals clearly confirm the presence of bacterial compounds bounded on the surface of Ag/SiO_2NC that affect protection and stability of the NC. The intense peaks around 3,431 and 2,914 cm^{-1} are attributed to the primary and secondary amines vibrations bands, respectively. The stretch C-N vibration of aliphatic amines existed at 1,078 cm^{-1} bands. These signals confirmed the presence of proteins in the Ag/SiO_2NC synthesis. Water bands were appeared at around 1,613 cm^{-1} corresponding to bending vibrations indicating the hygroscopic character of the powdered samples (Singh and Ahmed 2012). Si–O–Si and Si–OH absorptions bands have been observed at 1,078; 783; and 462 cm^{-1}. The Si–O–Ag linkages stretching were also seen at around 691 cm^{-1}. The band appears in the Ag/SiO_2NC suggesting bonding between the AgNPs and the oxygen bonded to SiO_2. The peaks 450 – 800 cm^{-1} are probably related to the pseudo-lattice vibrations (Mathur *et al.* 2006).

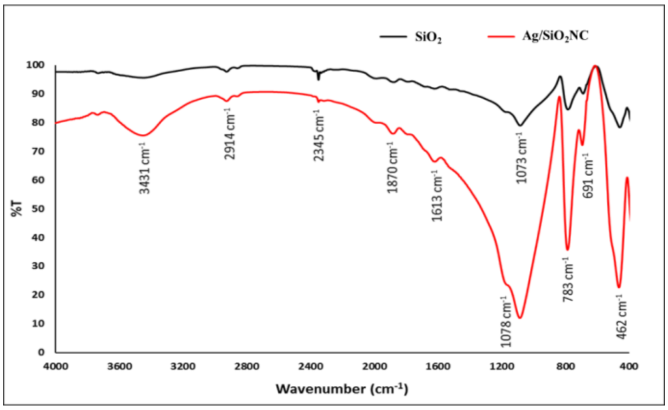

Fig. 3. The FTIR spectra of SiO_2 and Ag/SiO_2NC.

The Ag/SiO_2NC was examined by the TEM (Fig. 4) to investigate the morphology and size of the AgNPs (Fig. 4B). AgNPs are embedded within the matrix and on the surface of the SiO_2. TEM image showed small spherical shaped AgNPs having a diameter between 18 – 24 nm. Gu *et al.* (2011) reported that the AgNPs average particle size on the surfaces of SiO_2 had a little increase from 10 to 25 nm as reaction temperature increased. This should be attributed to the higher reduction rate of Ag^+ at the elevated reaction temperature.

SiO_2 has a net positive charge, while Ag/SiO_2NC may have a positive or negative surface charge depending on the surface functional group and solution pH (Jana *et al.* 2007; Jayasuriya 2017). The synthesis of Ag/SiO_2NC included binding primary amines as confirmed by the FTIR analysis. The primary amines were deprotonated during the bio-reduction process, were leading to a gradual decrease in the surface positive charge of SiO_2 and might approach zero (Jana *et al.* 2007). On the other hand, the binding between the AgNPs which are capped with highly negative proteins (El-Dein *et al.* 2021), and SiO_2 to give negatively charged Ag/SiO_2NC. The biosynthesized Ag/SiO_2NC had a negative charge, -31.0 mV (Fig. 5), which matched with Shanthil *et al.* (2012) results, -33 ± 2 mV and was better than Zhao *et al.* (2016) and El-Sheshtawy *et al.* (2020) results (-16.10 mV and -15 mV, respectively). Different studies (Verma and Stellacci 2010; Anas *et al.* 2013) have studied the interaction of charged nanomaterials with cells showing that positively charged nanomaterials have the greatest efficacy in penetrating the cell membrane. Other studies (Fuller *et al.* 2008; Martin *et al.* 2008) have examined the cellular uptake of negatively charged nanomaterials and proposed that negatively charged nanomaterials generate reactive oxygen species (ROS) contributes towards potent bacterial toxicity (Ivask *et al.* 2010; Agnihotri *et al.* 2013). A further study of the synthesized Ag/SiO_2NC should be taken into account to improve the antimicrobial efficacy of Ag/SiO_2NC to have a positive surface charge. The positive charge of the nanomaterials increases the efficient electrostatic interaction with the negative charges of the microbial cell wall (Li *et al.* 2011).

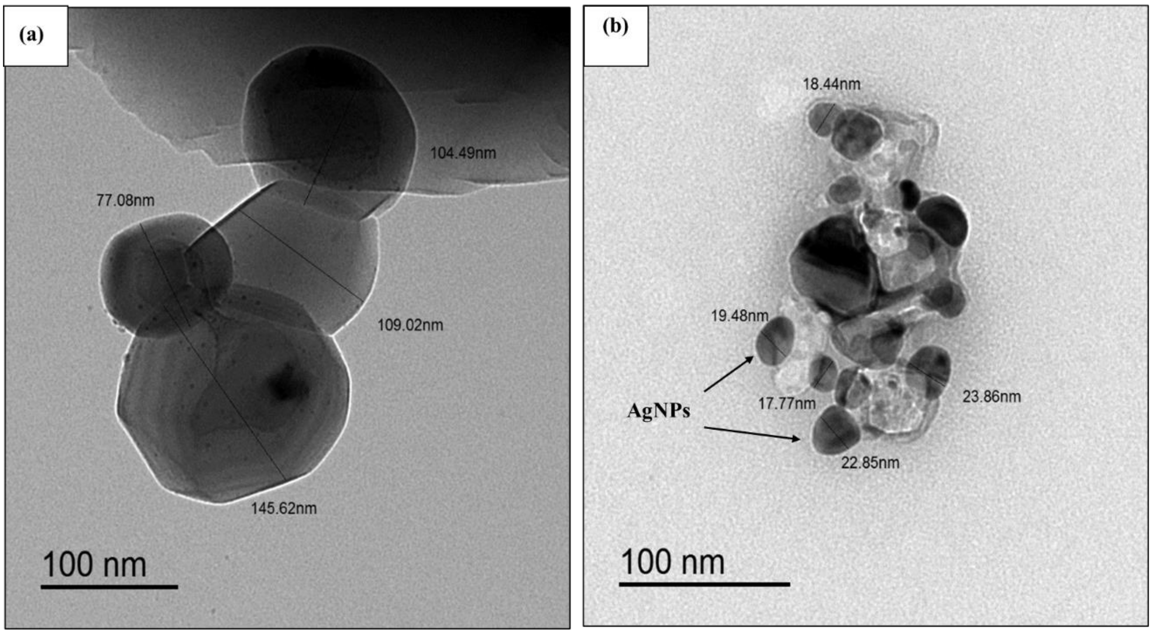

Fig. 4. (a) TEM micrograph of SiO_2. **(b)** TEM micrograph of Ag/SiO_2NC.

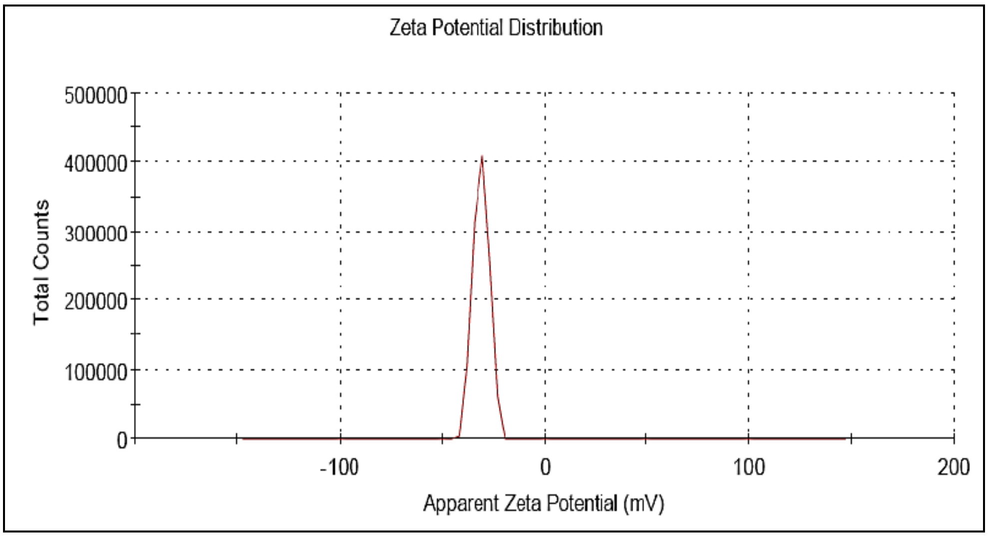

Fig. 5. Zeta potential measurement analysis of Ag/SiO_2NC (-31.0 mV).

Antimicrobial potential of Ag/SiO_2NC

The pathogenic bacteria, yeast, and fungi appeared to be more tolerant to SiO_2 than Ag/SiO_2NC. In this study, Ag/SiO_2NC was investigated to determine its antimicrobial action (Fig. 6 and Table 1). The NC revealed very good antimicrobial potential against a wide range of microorganisms such as *K. pneumoniae*, *S. aureus*, and *B. cinerea*. The inhibition of microbial growth due to surface contact with the SiO_2 nanocomposite containing AgNPs demonstrated that NC functionalized with the AgNPs has better antimicrobial action than bulk SiO_2. The antibacterial potential results of Ag/SiO_2NC in He et al. (2012) study revealed that Ag/SiO_2NC were sensitive to *S. aureus* and *E. coli* and with the inhibition zone diameter 15.3 mm and 10.4 mm, respectively. Lu et al. (2017) studied the combination between chlorhexidine and Ag/SiO_2NC and recorded that combination might produce synergistic bactericidal and candidacidal effects and improve the microbicidal efficiency. In addition, Ag/SiO_2NC showed antifungal potential against *B. cinerea* besides the antibacterial and anticandidal actions. Rodríguez-Cutiño *et al.* (2018) confirmed the antimicrobial properties of Ag/SiO_2NC against bacteria such as *E. coli*, *B. cereus*, *S. typhimurium*, and *S. aureus* in addition to the green squash fungi: *B. cinerea* and *R. solani*.

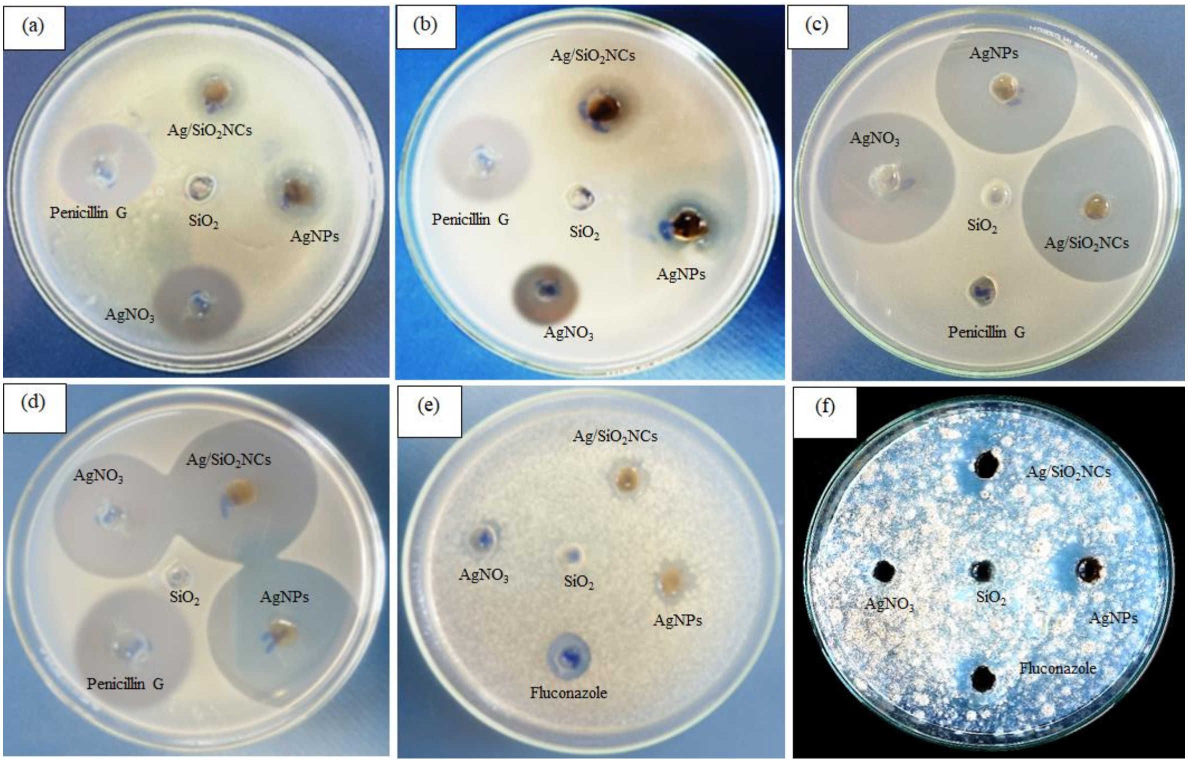

Fig. 6. Antimicrobial activity of SiO_2, AgNPs, and Ag/SiO_2NC; **(a)** *B. cereus*, **(b)** *E. coli*, **(c)** *K. pneumoniae*, **(d)** *S. aureus*, **(e)** *C. albicans*, and **(f)** *B. cinerea*.

Table 1. Antimicrobial activity of SiO_2, AgNPs and Ag/SiO_2NC against the pathogenic microbial strains (Highly significant = $^*P < 0.05$; $n = 3$).

Antibacterial activity (Inhibition zone, mm ± SD)				
Substance	***B. cereus***	***E. coli***	***K. pneumoniae***	***S. aureus***
$AgNO_3$	24 ± 0.06*	26 ± 0*	34 ± 0*	29 ± 0*
SiO_2	-ve	-ve	-ve	-ve
AgNPs	30 ± 0.14*	30 ± 0.14*	38 ± 0*	37 ± 0*
Ag/SiO2NC	20 ± 0.06*	22 ± 0.14*	36 ± 0*	34 ± 0*
Penicillin G potassium	29 ± 0*	30 ± 0*	-ve	26 ± 0.06*

Antifungal activity (Inhibition zone, mm ± SD)		
Substance	***C. albicans***	***B. cinerea***
$AgNO_3$	13 ± 0.06*	13 ± 0.14*
SiO_2	-ve	-ve
AgNPs	16 ± 0.06*	21 ± 0.14*
Ag/SiO2NC	14 ± 0.06*	24 ± 0.14*
Fluconazole	15 ± 0*	16 ± 0.14*

AgNPs and Penicillin G potassium showed a similar manner of MIC values (6.25 $\mu g.mL^{-1}$) against *S. aureus*, *B. cereus*, and *E. coli* compared to Ag/SiO_2NC (MIC value, 125 $\mu g.\ mL^{-1}$). The

MIC values against *B. cinerea* were 6.25 and 25 µg.mL^{-1} for Ag/SiO_2NC and fluconazole, respectively. The better growth inhibition percentage of Ag/SiO_2NC was against *B. cinerea* (50.2 %) followed by *B. cereus* (31.1 %), *S. aureus* (30.7 %), *E. coli* (26.6 %), and *C. albicans* (6.6 %) showing a dose-dependent manner of Ag/SiO_2NC antimicrobial action (Fig. 7). The minimum antibacterial concentration of the Ag/SiO_2NC is 0.2 and 0.3 µg.mL^{-1} for *Bacillus* sp. and *E. coli*, respectively (Huang 2008). Qasim *et al.* (2015) suggested Ag/SiO_2NC to be a potential antifungal agent for *C. albicans* 077 showing that this tested human pathogenic fungus was sensitive to Ag/SiO_2NC with MIC~6 µg.mL^{-1} of Ag/SiO_2NC. Vladkova *et al.* (2020) presented that TiO_2/SiO_2/Ag nanocomposite totally inhibited the *E. coli* growth within 30 min to 2 h. The growth of *B. cinerea* was almost completely inhibited (98.4 %) by Ag/SiO_2NC (6.4 µg.mL^{-1}) treatment compared with AgNPs alone (72.43 %, 6.4 µg.mL^{-1} as reported by Kim (2011).

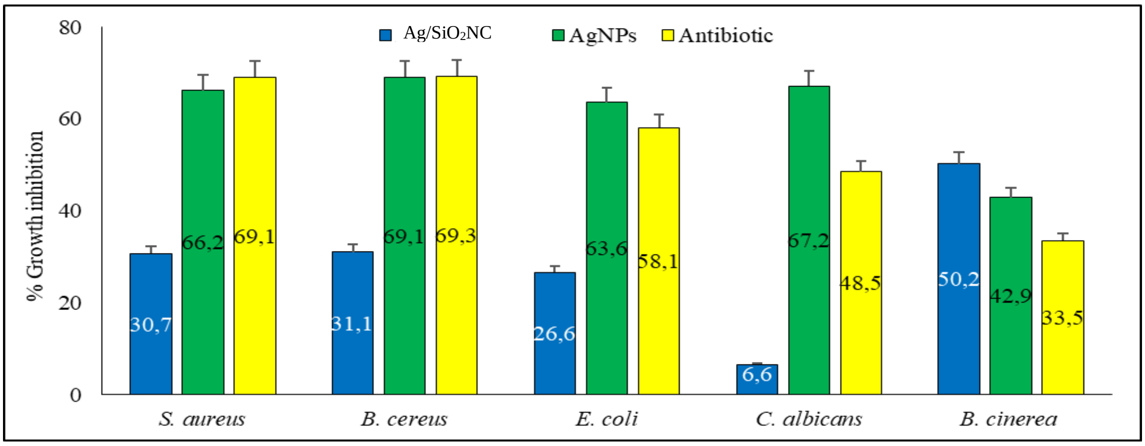

Fig. 7. Growth inhibition percentage of Ag/SiO_2NC, AgNPs, and antibiotics at MIC values against *S. aureus*, *B. cereus*, *E. coli*, *C. albicans*, and *B. cinerea*.

It is known that both, Ag^+ and AgNPs are effective antimicrobial agents even though their antimicrobial mechanism is not fully understood (Kędziora *et al.* 2018). Several studies (Feng *et al.* 2000; Lara *et al.* 2011) reported the different mechanism of the antimicrobial action of nanomaterials such as penetrating the cell wall and plasma membrane, ending with damaging DNA molecules. Others suggested that nanomaterials might interact with thiol groups in proteins, which induces the inactivation of microbial proteins. In the presented study, AgNPs bonded on the surface of SiO_2 have an opposite charge with Gram-positive bacteria, in that way killing them more easily than Gram-negative bacteria due to the electrostatic attraction.

The antimicrobial activities of Ag/SiO_2NC are investigated using *E. coli* and *B. cinerea* as two model microorganisms. As shown in Fig. 8, untreated *E. coli* was typically rod-shaped with smooth and intact cell walls. After being treated with Ag/SiO_2NC, cell walls became wrinkled and damaged. The separation between the bacterial cell wall and cell membrane was also noted.

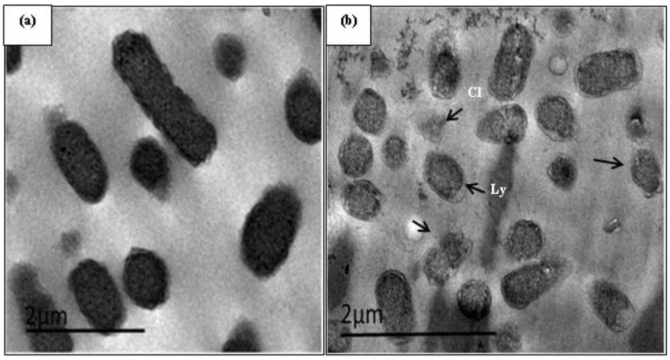

Fig. 8. The antibacterial action of Ag/SiO_2NC on the ultrastructure of *E. coli*. **(a)** A negative control (without Ag/SiO_2NC). **(b)** A treated sample (150 µg.mL^{-1}), there are irregular rods (arrows) with lysed cell walls (Ly) and complete cell lysis (Cl). Also, note the separation that occurs between the bacterial cell wall and cell membrane.

With treated *B. cinerea* (Fig. 9), TEM micrographs showed many changes, including the reduced size of treated cells, the formation of a mucilage matrix connecting the hyphal cells together, the appearance of big vacuole and lipid droplets with severe leakage of cytoplasmic contents in comparing to the control. The separation between the fungal cell wall and plasma membrane was also detected in the treated cells. The observed damages of the *E. coli* and *B. cinerea* cells after the treatment by Ag/SiO_2NC could be because of cellular interactions with the AgNPs. The combined action of adhesion and penetration of AgNPs might illustrate the biocidal action of the NC, plasma membrane being the target of rapid antimicrobial action of AgNPs in *E. coli* and *B. cinerea* (Rai *et al.* 2012). Eckhardt *et al.* (2013) reported that the binding of AgNPs with microbial proteins might inactivate the electron transport chain, in that way suppressing the respiration and growth of the microbial cells. To establish that the advantages of silver nanocomposites (AgNCs) and the possible mechanisms of their antimicrobial action outweigh the possible risks, the toxicity of AgNPs and AgNCs must be investigated.

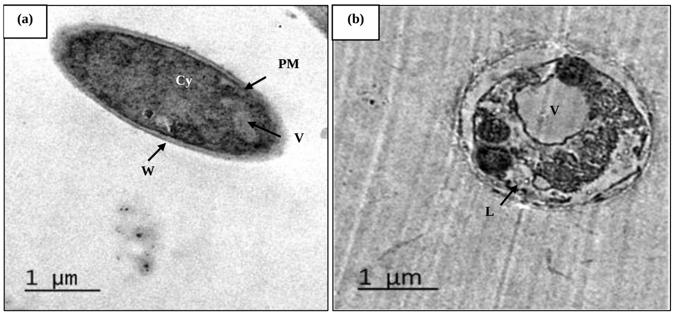

Fig. 9. The antifungal activity of Ag/SiO_2NC on the ultrastructure of *B. cinerea*. **(a)** negative control (without Ag/SiO_2NC). Note normal cell wall (W), plasma membrane (PM), Vacuole (V), and compact cytoplasm (Cy). **(b)** The treated sample, note, the big vacuole (V) and lipid droplets (L). Also, note the separation that occurs between the fungal cell wall and plasma membrane (arrow).

Conclusion

The embedded AgNPs in Ag/SiO_2NC mediated by *E. coli* D8 were characterized as negative-charged (-31.0 mV) and spherical with an average size ranging between 18 and 24 nm. Ag/SiO_2NC showed a good antimicrobial potential against Gram-negative and Gram-positive bacteria and pathogenic yeast and fungi. The Ag/SiO_2NC has brought many biomedical and agriculture applications (non-toxic to humans in minute concentrations). Further study will be designed to elucidate the mode of action of Ag/SiO_2NC as an antimicrobial agent.

Conflict of Interest

The authors declare that they have no conflict of interest.

References

Agnihotri S, Mukherji S, Mukherji S (2013) Immobilized silver nanoparticles enhance contact killing and show highest efficacy: elucidation of the mechanism of bactericidal action of silver. Nanoscale 5: 7328-7340.

Anas A, Jiya J, Rameez MJ, Anand PB, Anantharaman MR, Nair S (2013) Sequential interactions of silver–silica nanocomposite (Ag–SiO_2NC) with cell wall, metabolism and genetic stability of *Pseudomonas aeruginosa*, a multiple antibiotic-resistant bacterium. Lett. Appl. Microbiol. 56: 57-62.

Awwad AM, Salem NM, Aqarbeh MM, Abdulaziz FM (2020) Green synthesis, characterization of silver sulfide nanoparticles and antibacterial activity evaluation. Chem. Int. 6: 42-48.

Baheiraei N, Moztarzadeh F, Hedayati M (2012) Preparation and antibacterial activity of Ag/SiO_2 thin film on glazed ceramic tiles by sol–gel method. Ceram. Int. 38: 2921-2925.

Bozzola JJ (2007) Conventional specimen preparation techniques for transmission electron microscopy of cultured cells. *In* Walker JM (Eds.), Methods in Molecular Biology, Springer-Verlag, Berlin Heidelberg, pp. 1-18.

Chen K-J, Lin C-T, Tseng K-C, Chu L-K (2017) Using SiO_2-coated gold nanorods as temperature jump photothermal convertors coupled with a confocal fluorescent thermometer to study protein unfolding kinetics: a case of bovine serum albumin. J. Phys. Chem. C 121: 14981-14989.

Chhipa H, Joshi P (2016) Nanofertilisers, nanopesticides and nanosensors in agriculture. *In* Lichtfouse E (Eds.), Sustainable Agriculture Reviews, Springer-Verlag, Berlin Heidelberg, pp. 247-282.

Clinical and Laboratory Standards Document M2-A9 (2006) Performance standards for antimicrobial disk susceptibility tests: Approved standard- Ninth Edition, Clinical and Laboratory Standards Institute, Wayne, Pennsylvania, USA.

Clinical Laboratory Standards Document M27-A3 (2008) Reference method for broth dilution antifungal susceptibility testing of yeasts: Approved Standard-Third Edition, Clinical and Laboratory Standards Institute, Wayne, Pennsylvania, USA.

Clinical and Laboratory Standards Document M100-S26 (2017) Performance standards for antimicrobial susceptibility testing: Approved standard- twenty-seven Edition, Clinical and Laboratory Standards Institute, Wayne, Pennsylvania, USA.

Das NM, Singh AK, Ghosh D, Bandyopadhyay D (2019) Graphene oxide nanohybrids for electron transfer-mediated antimicrobial activity. Nanoscale Adv. 1: 3727-3740.

Diagne A, Diop BN, Andreazza C, Sembène M (2020) Optimization of silver@ silica nanoparticles for better antimicrobial effeceincy. J. Global Biosci. 9: 6796-6806.

Duan H, Wang D, Li Y (2015) Green chemistry for nanoparticle synthesis. Chem. Soc. Rev. 44: 5778-5792.

Eckhardt S, Brunetto PS, Gagnon J, Priebe M, Giese B, Fromm KM (2013) Nanobio silver: its interactions with peptides and bacteria, and its uses in medicine. Chem. Rev. 113: 4708-4754.

Egger S, Lehmann RP, Height MJ, Loessner MJ, Schuppler M (2009) Antimicrobial properties of a novel silver-silica nanocomposite material. Appl. Environ. Microbiol. 75: 2973-2976.

El-Dein MMN, Baka ZAM, Abou-Dobara MI, El-Sayed AKA, El-Zahed MM (2021) Extracellular biosynthesis, optimization, characterization and antimicrobial potential of *Escherichia coli* D8 silver nanoparticles. J. Microbiol. Biotechnol. Food Sci. 10: 648-656.

El-Sheshtawy HS, Shoueir KR, El-Kemary M (2020) Activated H_2O_2 on Ag/SiO_2–$SrWO_4$ surface for enhanced dark and visible-light removal of methylene blue and p-nitrophenol. J. Alloys Comp. 842: 155848.

El-Zahed MM, Baka Z, Abou-Dobara MI, El-Sayed A (2021) *In vitro* biosynthesis and antimicrobial potential of biologically reduced graphene oxide/Ag nanocomposite at room temperature. J. Microbiol. Biotechnol. Food Sci. 10: e3956–e3956.

Enan ET, Ashour AA, Basha S, Felemban NH, El-Rab SMFG (2021) Antimicrobial activity of biosynthesized silver nanoparticles, amoxicillin, and glass-ionomer cement against *Streptococcus mutans* and *Staphylococcus aureus*. Nanotechnol. 32: 215101.

Feng QL, Wu J, Chen GQ, Cui FZ, Kim TN, Kim JO (2000). A mechanistic study of the antibacterial effect of silver ions on *Escherichia coli* and *Staphylococcus aureus*. J. Biomed. Mat. Res. 52: 662-668.

Fuller JE, Zugates GT, Ferreira LS, Ow HS, Nguyen NN, Wiesner UB, Langer RS (2008) Intracellular delivery of core–shell fluorescent silica nanoparticles. Biomater. 29: 1526-1532.

Gankhuyag S, Bae DS, Lee K, Lee S (2021) One-pot synthesis of SiO_2@Ag mesoporous nanoparticle coating for inhibition of *Escherichia coli* bacteria on various surfaces. Nanomater. 11: 549.

Granbohm H, Larismaa J, Ali S, Johansson L-S, Hannula S-P (2018) Control of the size of silver nanoparticles and release of silver in heat treated SiO_2-Ag composite powders. Mater. 11: 80.

Gu G, Xu J, Wu Y, Chen M, Wu L (2011) Synthesis and antibacterial property of hollow SiO_2/Ag nanocomposite spheres. J. Colloid Interface Sci. 359: 327-333.

Hamad A, Khashan KS, Hadi A (2020) Silver nanoparticles and silver ions as potential antibacterial agents. J. Inorg. Organomet. Polym. Mater. 1-18.

He Q, Wu Z, Huang C, Zeng X (2012) Preparation and characterization of silver loaded antibacterial nanosilica particles. Advanced Science Letters, 10: 177-181.

Huang L, Jin K, Deng B (2008) Research into SiO_2/Ag composite material. Jiangxi Science 5.

Ivask A, Bondarenko O, Jepihhina N, Kahru A (2010) Profiling of the reactive oxygen species-related ecotoxicity of CuO, ZnO, TiO_2, silver and fullerene nanoparticles using a set of recombinant luminescent *Escherichia coli* strains: differentiating the impact of particles and solubilised metals. Anal. Bioanal. Chem. 398: 701-716.

Jana NR, Earhart C, Ying JY (2007) Synthesis of water-soluble and functionalized nanoparticles by silica coating. Chem. Mater. 19: 5074-5082.

Jayasuriya CK (2017) Interfacial bonding in polymer–ceramic nanocomposites. Reference Module in Materials Science and Materials Engineering. Elsevier Inc.

Kędziora A, Speruda M, Krzyżewska E, Rybka J, Łukowiak A, Bugla-Płoskońska G (2018) Similarities and differences between silver ions and silver in nanoforms as antibacterial agents. Int. J. Mol. Sci. 19: 444.

Kim H-J, Park H-J, Choi S-H (2011) Antimicrobial action effect and stability of nanosized silica hybrid Ag complex. J. Nanosci. Nanotechnol.11: 5781-5787.

Krishnaraj C, Ramachandran R, Mohan K, Kalaichelvan PT (2012) Optimization for rapid synthesis of silver nanoparticles and its effect on phytopathogenic fungi. Spectrochim. Acta Part A: Mol. Biomol.Spectrosc. 93: 95-99.

Lara HH, Garza-Treviño EN, Ixtepan-Turrent L, Singh DK (2011) Silver nanoparticles are broad-spectrum bactericidal and virucidal compounds. J. Nanobiotechnol. 9: 1-8.

Li M, Zhang L, Zhang Z, Shi J, Liu Y, Chen J, Sun N, Wei W (2021) SiO_2-coated Ag nanoparticles for conversion of terminal alkynes to propolic acids via CO_2 insertion. ACS Appl. Nano Mater. 4: 7107-7115.

Li W-R, Xie X-B, Shi Q-S, Duan S-S, Ouyang Y-S, Chen Y-B (2011) Antibacterial effect of silver nanoparticles on *Staphylococcus aureus*. Biometals 24: 135-141.

Lu M-M, Wang Q-J, Chang Z-M, Wang Z, Zheng X, Shao D, Dong W-F, Zhou Y-M (2017) Synergistic bactericidal activity of chlorhexidine-loaded, silver-decorated mesoporous silica nanoparticles. Int. J. Nanomed. 12: 3577-3589.

Martin AL, Bernas LM, Rutt BK, Foster PJ, Gillies ER (2008) Enhanced cell uptake of superparamagnetic iron oxide nanoparticles functionalized with dendritic guanidines. Bioconjug. Chem.19: 2375-2384.

Mathur S, Shen H, Veith M, Rapalaviciute R, Agne T (2006) Structural and optical properties of highly Nd-doped yttrium aluminum garnet ceramics from alkoxide and glycolate precursors. J. Am. Ceram. Soc. 89: 2027-2033.

Musere PSF, Rahman A, Uahengo V, Naimhwaka J, Likius D, Bhaskurani SVHS, Jonnalagadda SB (2021) Synthesis of silver nanoparticles using pearl millet (*Pennisetum Glaucum*) husk and its application for the removal of algae in the water and catalytic oxidation of benzyl alcohol. J. Clean. Prod. 127581.

Narayanan KB, Sakthivel N (2011) Green synthesis of biogenic metal nanoparticles by terrestrial and aquatic phototrophic and heterotrophic eukaryotes and biocompatible agents. Adv. Colloid Interface Sci. 169: 59-79.

Nguyen HC, Nguyen TT, Dao TH, Ngo QB, Pham HL, Nguyen TBN (2016). Preparation of Ag/SiO_2 nanocomposite and assessment of its antifungal effect on soybean plant (a *Vietnamese* species DT-26). Adv. Natural Sci.: Nanosci. Nanotechnol. 7: 45014.

Oh S-D, Lee S, Choi S-H, Lee I-S, Lee Y-M, Chun J-H, Park, H-J (2006). Synthesis of Ag and Ag-SiO_2 nanoparticles by γ-irradiation and their antibacterial and antifungal efficiency against *Salmonella enterica* serovar *Typhimurium* and *Botrytis cinerea*. Colloids Surf.A: Physicochem. Eng. Asp. 275: 228-233.

Ouda SM (2014) Antifungal activity of silver and copper nanoparticles on two plant pathogens, *Alternaria alternata* and *Botrytis cinerea*. Res. J. Microbiol. 9: 34.

Pareek V, Devineau S, Sivasankaran SK, Bhargava A, Panwar J, Srikumar S, Fanning S (2021) Silver nanoparticles induce a triclosan-like antibacterial action mechanism in multi-drug resistant *Klebsiella pneumoniae*. Front. Microbiol.12: 183.

Parveen K, Banse V, Ledwani L (2016) Green synthesis of nanoparticles: their advantages and disadvantages. AIP Conference Proceedings *1724*: 020048.

Qasim M, Singh BR, Naqvi AH, Paik P, Das D (2015) Silver nanoparticles embedded mesoporous SiO_2 nanosphere: an effective anticandidal agent against *Candida albicans* 077. Nanotechnol. 26: 285102.

Rai MK, Deshmukh SD, Ingle AP, Gade AK (2012) Silver nanoparticles: the powerful nanoweapon against multidrug-resistant bacteria. J. Appl. Microbiol. 112: 841-852.

Rodríguez-Cutiño G, Gaytán-Andrade JJ, García-Cruz A, Ramos-González R, Chávez-González ML, Segura-Ceniceros EP, Martínez-Hernández JL, Govea-Salas M, Ilyina A (2018) Nanobiotechnology approaches for crop protection. In Kumar V, Kumar M, Prasad R (Eds.), Phytobiont and ecosystem restitution, Springer, Singapore, pp. 1-21.

Sadeghi B, Ghammamy S, Sedaghat S (2013) Synthesis and characterization of silver-silica heterogeneous nanocomposite particles by lithium aluminum hydroxide reducing method. Int. J. Nano Dimens. 3: 271-279.

Shanthil M, Thomas R, Swathi RS, George TK (2012). Ag@SiO_2 core–shell nanostructures: distance-dependent plasmon coupling and SERS investigation. J. Phys. Chem. Let.3: 1459-1464.

Sharma P, Teixeira de Mattos MJ, Hellingwerf KJ, Bekker M (2012) On the function of the various quinone species in *Escherichia coli*. FEBS 279: 3364-3373.

Si Y, Li L, Qin X, Bai Y, Li J, Yin Y (2019) Porous SiO_2-coated Au-Ag alloy nanoparticles for the alkyne-mediated ratiometric Raman imaging analysis of hydrogen peroxide in live cells. Anal. Chimic. Acta 1057: 1-10.

Singh V, Ahmed S (2012) Silver nanoparticle (AgNPs) doped gum acacia–gelatin–silica nanohybrid: An effective support for diastase immobilization. Int. J. Biol. Macromolec. 50: 353-361.

Sohrabnezhad S, Jafarzadeh A, Rassa M (2020) Antibacterial activity of mesoporous silica nanofibers. Iranian Journal of Chem. Chem. Eng. 39: 1-11.

Takamiya AS, Monteiro DR, Gorup LF, Silva EA, de Camargo ER, Gomes-Filho JE, de Oliveira SHP, Barbosa DB (2021) Biocompatible silver nanoparticles incorporated in acrylic resin for dental application inhibit *Candida albicans* biofilm. Mater. Sci. Eng.C 118: 111341.

Verma A, Stellacci F (2010) Effect of surface properties on nanoparticle–cell interactions. Small 6: 12-21.

Vladkova T, Angelov O, Stoyanova D, Gospodinova D, Gomes L, Soares A, Mergulhao F, Ivanova I (2020) Magnetron co-sputtered TiO_2/SiO_2/Ag nanocomposite thin coatings inhibiting bacterial adhesion and biofilm formation. Surf. Coat. Technol. 384: 125322.

Xu C, Li W, Wei Y, Cui X (2015) Characterization of SiO_2/Ag composite particles synthesized by *in situ* reduction and its application in electrically conductive adhesives. Mater. Des.83: 745-752.

Xu K, Wang J-X, Kang X-L, Chen J-F (2009) Fabrication of antibacterial monodispersed Ag–SiO_2 core–shell nanoparticles with high concentration. Mater. Let. 63: 31-33.

Yang C, Jian R, Huang K, Wang Q, Feng B (2021) Antibacterial mechanism for inactivation of *E. coli* by AgNPs@ polydoamine/titania nanotubes via speciation analysis of silver ions and silver nanoparticles by cation exchange reaction. Microchem. J. 160: 105636.

Youssef K, Roberto SR (2021) Chitosan/silica nanocomposite-based formulation alleviated gray mold through stimulation of the antioxidant system in table grapes. Int. J. Biol. Macromol. 168: 242-250.

Zaferani SH (2018) Introduction of polymer-based nanocomposites. *In* Kawaid M, Khan MM (Eds.), Polymer-based nanocomposites for energy and environmental applications, Springer-Verlag, Berlin Heidelberg, pp. 1-25.

Zhang H, Chen S, Jia X, Huang Y, Ji R, Zhao L (2021) Comparation of the phytotoxicity between chemically and green synthesized silver nanoparticles. Sci. Total Environ. 752: 142264.

Zhao K, Rong G, Hao Y, Yu L, Kang H, Wang X, Wang X, Jin Z, Ren Z, Li Z (2016) IgA response and protection following nasal vaccination of chickens with Newcastle disease virus DNA vaccine nanoencapsulated with Ag@SiO_2 hollow nanoparticles. Sci. Rep. 6: 1-12.